Nerve Injury Induces a Rapid Efflux of Nitric Oxide (NO) Detected with a Novel NO Microsensor

Shanta M. Kumar,[1] D. Marshall Porterfield,[4] Kenneth J. Muller,[3] Peter J. S. Smith,[2] and Christie L. Sahley[1]

[1]Department of Biological Sciences, Purdue University, West Lafayette, Indiana 47907, [2]BioCurrents Research Center, Marine Biological Laboratory, Woods Hole, Massachusetts 02543, [3]Department of Physiology and Biophysics and Neuroscience Program, University of Miami School of Medicine, Miami, Florida 33136, and [4]Department of Biological Sciences, University of Missouri at Rolla, Rolla, Missouri 65409

An early step in repair of the leech CNS is the appearance of endothelial nitric oxide synthase (eNOS) immunoreactivity and NOS activity, but coincident generation of NO at the lesion after injury has not been shown. This is important because NO can regulate microglial cell motility and axon growth. Indirect measurement of NO with the standard citrulline assay demonstrated that NO was generated within 30 min after nerve cord injury. A polarographic NO-selective self-referencing microelectrode that measures NO flux noninvasively was developed to obtain higher spatial and temporal resolution. With this probe, it was possible to demonstrate that immediately after the leech CNS was injured, NO left the lesion with a mean peak efflux of 803 ± 99 fmol NO cm^{-2} sec^{-1}. NO efflux exponentially declined to a constant value, as described through the equation $f(t) = y_o + ae^{-t/\tau}$, with $\tau = 117 \pm 30$ sec. The constant $y_o = 15.8 \pm 4.5$ fmol cm^{-2} represents a sustained efflux of NO. Approximately 200 pmol NO cm^{-2} is produced at the lesion ($n = 8$). Thus, injury activates eNOS already present in the CNS and precedes the accumulation of microglia at the lesion, consistent with the hypothesis that NO acts to stop the migrating microglia at the lesion site.

Key words: nitric oxide (NO); microglia; nerve injury; NO-selective microsensor; NO efflux; endothelial nitric oxide synthase (eNOS); leech CNS; regeneration; nerve repair

CNS injury triggers a cascade of sequential cellular events, but repair is ordinarily incomplete in mammals (Brecknell and Fawcett, 1996). In contrast, the sequence of cellular events after neuronal injury in the leech CNS leads to successful regeneration of axons, repair of synaptic connections, and restoration of function (Nicholls, 1987; Modney et al., 1997). The microglial cells are important elements of the repair process. Significantly, their migration to and stopping at the site of injury appear to be regulated by nitric oxide (NO) (Chen et al., 2000). Nitric oxide synthase (NOS) activity at the lesion is one of the earliest events after crushing or cutting the leech nerve cord (Shafer et al., 1998), whereas in mammals, NOS activity reportedly appears only after hours or days. Nevertheless, few measurements of NO release at lesions have been attempted in other animal species.

Several types of cells express NOS in response to injury and are assumed to produce NO. In all nervous systems that have been examined, microglial cells and macrophages are one source of NO (Banati et al., 1993). The inducible form (iNOS) reported for mammals has not been described for leech. Microglia, glia, and nerve-associated muscle cells in leech express active endothelial NOS (eNOS), beginning within 5 min after injury (Shafer et al., 1998), as some muscle cells do in mammals (Cobbs et al., 1997). Although neuronal–brain (nNOS) activity has not been described specifically at lesions, nNOS appears or increases in various neurons after injury (Fiallos-Estrada et al., 1993; Vizzard et al., 1995; Yu, 1997).

Several techniques are currently available for the detection of NO, perhaps the best established being the citrulline assay (Bredt and Schmidt, 1996). This approach, although suitable for demonstrating the activity of NOS, has limited spatial resolution. To localize the production of NO with a spatial resolution of millimeters or micrometers, a microsensor is required. We have modified existing designs, as described in Materials and Methods, to produce an NO-selective microelectrode from carbon fibers with diameters as small as 5 μm (Cahill and Wightman, 1995) that combines sensitivity and selectivity with ease of manufacturing. The reactive surface of this design is 28 μm^2. Furthermore, the microsensor is used in a self-referencing mode (Smith, 1995; Smith et al., 1999), allowing continuous measurement of flux and flux patterns without the influence of drift and instabilities. The result is a robust new method for monitoring the diffusion of NO away from a source, in this case, the damaged nervous system of the leech. Preliminary results have also demonstrated sensitivity at the single cell level (Porterfield et al., 2000).

Portions of this work have been published previously in abstract form (Kumar et al., 1999).

MATERIALS AND METHODS

Preparation and operations. Adult 4–6 gm adult leeches (*Hirudo medicinalis*) were obtained from a commercial supplier (Leeches USA, Westbury, NY) and maintained in artificial pond water (Forty Fathoms, 0.5 gm/l H_20; Marine Enterprises, Towson, MD) at 22°C. For experiments,

Received May 12, 2000; revised Oct. 2, 2000; accepted Oct. 11, 2000.

This work was supported by National Institutes of Health Grants NS34927 and NS37025 to K.J.M. and C.L.S., National Center for Research Resources Grant P41 RR01395 to P.J.S.S., and the Graduate Assistance in Areas of National Need training grant to S.M.K. We thank Dr. Don Ready for use of his laboratory to perform the citrulline assays, Dr. Sandra Rossie for help and the use of her scintillation counter, Kasia Hammar and family for their hospitality to S.M.K. during her visit to the BioCurrents Research Center, Rick Sanger for help with the NO selective probe, and Jane A. McLaughlin for help in coordinating our collaboration. In addition, we are grateful to Drs. Ken Robinson, Joe Vanable, and Mark Messerli for useful suggestions and to Dr. John Burnger for his help in analyzing the data.

Correspondence should be addressed to Dr. Christie L. Sahley, Department of Biology, B326 Lilly Hall, 1392 State Street, Purdue University, West Lafayette, IN 47907. E-mail: csahley@bilbo.bio.purdue.edu.

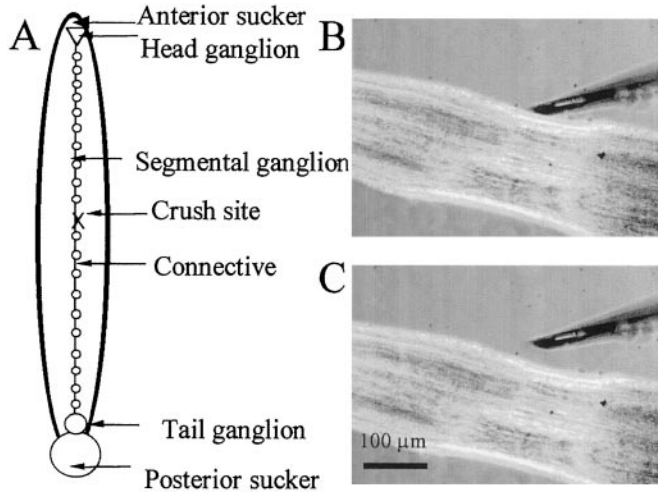

Figure 1. Diagram of the leech, showing the site of crushing the nerve cord, and the recording arrangement. *A*, The CNS of *Hirudo medicinalis* consists of head and tail ganglia and 21 segmental ganglia. Each segmental ganglion contains >400 cell bodies and is linked to its neighbors by thousands of axons that form the connectives. Connectives were injured by crushing with forceps (Materials and Methods). *B*, *C*, Photographs of an injured leech nerve cord and the self-referencing NO probe. During measurements, the probe was moved orthogonally to the cord over a distance of 30 μm at a frequency of 0.3 Hz in a plane parallel to the surface of the culture dish. The probe was positioned at the injury site in *B*, whereas in *C* it was displaced 30 μm. Scale bar, 100 μm.

individual segmental ganglia with connectives were dissected in physiological saline (Nicholls and Baylor, 1968) from the animal as shown in Figure 1*A* and pinned in a dish coated with silicone rubber (Sylgard 184; Dow Corning, Midland, MI). The connectives were crushed with a pair of fine forceps (Dumont 5) after recording baseline levels with the NO probe, as shown in Figure 1, *B* and *C*.

Citrulline assay. Production of NO after injury was determined indirectly by measuring the conversion of [^{3}H]arginine to [^{3}H]citrulline using the NOS detect Assay Kit (catalog #204500; Stratagene, La Jolla, CA). For an uninjured control condition, an entire nerve cord was dissected from an adult leech and incubated 30 min at room temperature. In the experimental, injured preparation, an entire adult nerve cord was similarly dissected, but the connectives were injured with forceps between all ganglia before incubation for 30 min at room temperature. Then each nerve cord was flash-frozen in liquid N_2 and homogenized in buffer containing 25 mM Tris-HCl, pH 7.4, 1 mM EDTA, and 10 mM EGTA (Sigma, St. Louis, MO). The tissue homogenate was kept on ice, pipetted into 1.5 ml Eppendorf tubes, and spun at 14,000 × *g* for 5 min at 4°C. NOS activity was measured in the supernatant. To verify that all samples contained equal amounts of tissue extract, protein assays were performed on similarly treated injured and uninjured tissue using the *dotMetric* Protein Assay Kit (catalog #2030; Chemicon, Temecula, CA).

A reaction mixture containing 250 μl of 2× reaction buffer, 50 μl of 10 mM NADPH, 10 μl of L-2,3,4,5-[^{3}H]arginine monohydrochloride TRK698 (1 μCi/μl) (Amersham Pharmacia Biotech, Piscataway, NJ), 50 μl of 6 mM $CaCl_2$, and 40 μl of H_2O was stored on ice. For each reaction, 40 μl of reaction mixture was combined with 10 μl of tissue extract. The positive control consisted of 40 μl of reaction mixture added to 10 μl of rat cerebellum extract, previously demonstrated to contain NOS activity (Bredt and Snyder, 1990). As a negative control, 5 μl of the inhibitor N^{ω}-nitro-L-arginine methyl ester hydrochloride (L-NAME) (Sigma) was added to 40 μl of reaction buffer before adding 10 μl of tissue extract. Each reaction was incubated 30 min in reaction buffer at 25°C. The reactions were stopped by adding 400 μl of stop buffer containing 50 mM HEPES, pH 5.5, and 5 mM EDTA. Equilibrated resin (100 μl) was added to each reaction sample, and the reaction samples were spun at 14,000 × *g* for 30 sec at 4°C. The [^{3}H]citrulline in the eluate was measured as thousands of counts per minute using a 1450 Microbeta Plus Liquid Scintillation Counter (Wallac, Gaithersburg, MD).

Nitric oxide microsensors. There are several designs of NO sensors, including one by Malinski and Taha (1992) that uses selective coatings of monomeric tetrakis (3-methoxy-4-hydroxyphenyl) porphyrin (Ni-TMPP) and Nafion over carbon to exclude reactants such as NO_2^- and ascorbate. The sensor can be flame-etched to a fine tip < 1 μm with a reactive surface of ~4 μm^2. These porphyrin electrodes have since been the method of choice in several tissue or single-cell NO studies ranging from smooth muscle cells, cardiac myocytes (Malinski and Taha, 1992; Balligand et al., 1994), and endothelial cells (Lantoine et al., 1998) to human platelets and osteoclasts (Malinski et al., 1993; Silverton et al., 1995). However, in several of these cases, the finely etched tip, which is difficult to make, has been abandoned for a more robust fiber design with larger reactive surfaces. Where spatial resolution was not critical, carbon fiber arrays with millimeter reactive lengths were used (Tschudi et al., 1996). Friedemann et al. (1996) developed an alternative to the porphyrin coating to produce NO selectivity in which Ni-TMPP is replaced by *o*-phenylenediamine (*o*-PD) to produce an electrode with excellent characteristics in terms of both sensitivity (35 ± 7 nM) and selectivity against NO_2^- and ascorbate. Unfortunately, that probe is relatively large, with a cylinder diameter of 30 μm and a reactive area of 10^4 μm^2.

For the measurements of nitric oxide in this study, a carbon fiber electrode was modified with *o*-PD and Nafion. This procedure combined the protocol of Friedemann et al. (1996), described above, with a fine carbon fiber described by Cahill and Wightman (1995), resulting in a sensitive and robust microsensor that was comparatively simple to build. The construction involved encasing a 5 μm carbon fiber (Amoco, Greenville, SC) in a glass microcapillary by heating and pulling the glass over the fiber (Sutter P97; Sutter Instrument Company, Novato, CA). The fiber was stabilized and sealed within the pulled pipette using Epoxylite (Epoxylite Corp., Westerville, OH) cured in an oven at 110°C for 5–10 hr. The electrode was backfilled with a graphite–epoxy paste (PX-grade Graphpoxy; Dylon Industries, Cleveland, OH), a copper wire was inserted to make electrical contact with the carbon fiber through the conductive paste, and the graphite–epoxy paste was cured for 5–10 hr at 110°C. The excess carbon fiber was chopped with a scalpel and beveled to 30°. Next, *o*-PD and Nafion were applied to the tip to impart selectivity for the oxidation of NO (Friedemann et al., 1996). Nafion is a polysulfonated Teflon that carries an intrinsic negative charge, repelling electrochemically active anions (nitrate, nitrite, and ascorbate). The *o*-PD coating is thought to impart selectivity to NO oxidation by size exclusion of noncharged interferents such as electrochemically active catecholamines. Nafion (5% in aliphatic alcohols; Aldrich, Milwaukee, WI) was applied in three coats that were each dried at 110°C for 5–10 min. The *o*-PD plating solution contained 5 mM *o*-phenylenediamine dihydrochloride (Sigma) with 100 mM ascorbic acid in 100 mM phosphate buffer, pH 7.4, and was freshly made for each plating session. The *o*-PD was plated at a constant +0.90 V potential until a stable current was obtained.

The modified carbon fiber electrodes (Fig. 2*A*) had final tip diameters of 7–8 μm and were operated with an Ag/AgCl return electrode that completed the circuit in solution via a 3 M KCl/5% agar bridge. The polarization voltage during operation was 0.90 V, and the electrode was operated in self-referencing mode as described below and for the self-referencing oxygen microelectrode (Land et al., 1999). Before and after use, the electrode was calibrated as described by Friedemann et al. (1996) against known concentrations of NO (Fig. 2*B*, see also below) and tested for specificity against ascorbic acid.

The technique was validated with gradients created by the NO donor *S*-nitroso-*N*-acetylpenicillamine (SNAP) (Lander et al., 1993). A source micropipette (diameter, 10 μm) was filled with a 0.5% agar solution containing 11.4 mM SNAP in phosphate buffer, pH 7.4. The gelled source was maintained in a dish containing phosphate buffer. The gradient was characterized and modeled so that measured NO flux values could be compared with theoretically derived values as done during the validation of the self-referencing electrochemical detection of oxygen (Land et al., 1999). As described in more detail below, a self-referencing electrode made two measurements at known distances apart, with its analog signal digitized and processed by computer. The derived differential value was converted to a flux measurement. Because the electrode was constrained in the time that it remained at each position, underestimates were theoretically possible because of limitations on response time. This was a concern with the original Seris probes (Smith et al., 1999), but not with electrochemical devices having shorter response times down to the range of tens or hundreds of milliseconds, such as probes of the present design (Friedemann et al., 1996; Porterfield et al., 2000). Therefore, no correction factor was required with the nitric oxide sensor operating as a self-referencing probe at a step frequency of 0.3 Hz.

Experimental setup for NO measurement. The experimental setup for

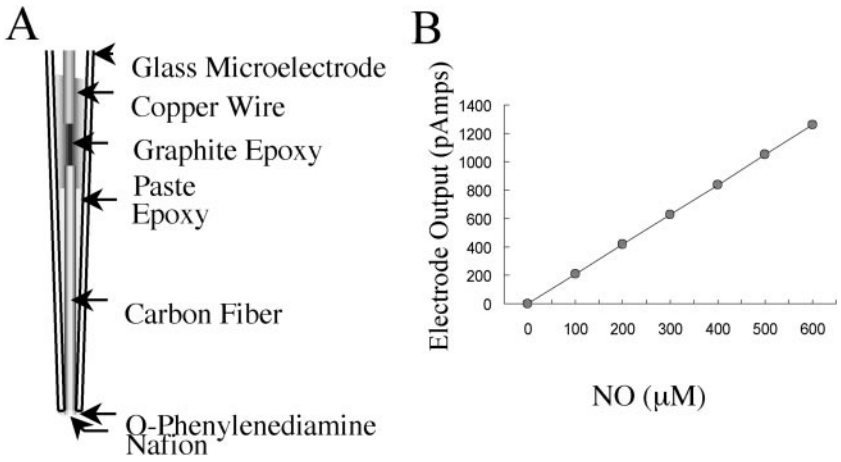

Figure 2. Construction and calibration of the NO-selective microelectrode. *A*, The electrode body was constructed by pulling a heated glass microcapillary around a 5 μm carbon fiber. The fiber was then sealed into the micropipette with epoxy. A copper wire was connected to the fiber by filling the back of the electrode with graphite paste. The tip was finished by beveling it, coating with Nafion, and plating with *o*-phenylenediamine. *B*, Before each experiment, the electrode was calibrated with a series of known concentrations of NO, and its selectivity was tested against ascorbic acid. The slope *S* of this calibration curve was used to calculate the flux of NO released at the injury site according to the Fick equation (see Materials and Methods).

measuring the flux of nitric oxide with a self-referencing microsensor was similar to that originally described for the self-referencing ion-selective (Seris) electrodes (Smith, 1995; Smith et al., 1999) and recently modified for electrochemical microsensors (Land et al., 1999). The rig was constructed around an Axiovert 10 inverted microscope (Zeiss, Oberkochen, Germany) fitted with a stage plate on which the head-stage and translational motion control system were mounted. The latter consisted of Newport 310 series translation stages arranged in an orthogonal array and driven by size 23 linear stepper motors. This arrangement provided nanometer resolution of movement for the electrode over micrometers in either the square-wave measurement translation or single-step positional mode (Smith et al., 1999). A computer with IonView software controlled movement. The entire assembly was mounted on an antivibration table and housed within a Faraday box. This box was thermally insulated and equipped with a temperature control system. The motion controllers, temperature controllers, head-stage, main amplifiers, and controlling software were products of the BioCurrents Research Center (Marine Biological Laboratory, Woods Hole, MA; *www.mbl.edu/BioCurrents*).

Direct measurement of NO flux. Direct measurement of NO flux is based on the translational movement of the microsensor at a given frequency through a gradient of NO. The movement of NO through the extracellular medium by diffusion can be described by Fick's Law. In this relationship the flux is expressed as pmol cm^{-2} sec^{-1} and given as $J = -D\Delta C/\Delta r$, where D is the diffusion coefficient for NO ($2.6 \cdot 10^{-5}$ cm^{-2} sec^{-1}), ΔC is the concentration difference between the two measurement positions (pmol cm^{-3}), and Δr is the excursion distance of the sensor (in this application, 30 μm). The differential current measured by the electrode was converted into a concentration, as discussed by Land et al. (1999) for oxygen.

In situ *measurement of NO.* Before every experiment, the electrode was calibrated against known concentration gradients of NO. A standard 2 mM $NO^{\bullet}$ solution for calibration was made by bubbling $NO^{\bullet}$ gas (Matheson Gas Products, Secaucus, NJ) to saturation in saline purged of O_2 with Ar gas (Gevantman, 1995). In each experiment the slope of the linear calibration curves (Fig. 2*B*) and the difference in current (I) measured experimentally at two measurement positions 30 μm apart (Fig. 1*B*,*C*) were used to calculate the mean flux of nitric oxide from the injury site according to the flux relationship described above and the procedure in Land et al. (1999). The differential current measured in response to the 0.9 V polarization was directly proportional to the concentration of NO.

During measurements, the probe was moved orthogonally to the cord in a plane parallel to the surface of the recording dish, a standard 35 mm tissue culture dish (Falcon, Oxnard, CA) partly filled with Sylgard 184 silicone rubber (Dow Corning, Midland, MI). The Sylgard-filled dishes were partially cured overnight at room temperature, baked 2 hr at 60°C, and soaked in distilled water for at least 3 d before use. Four midbody leech ganglia with their connectives intact were dissected from the leech and pinned to the Sylgard in the culture dish with 0.10-mm-diameter minutien pins (Original Emil, Orly, Austria) in leech saline, pH 7.4 (Kuffler and Potter, 1964). In experiments to test the specificity of the response, the NOS inhibitor L-NAME and, as a control, its inactive enantiomer N^{ω}-nitro-D-arginine methyl ester (D-NAME) were used. Preparations were dissected and pinned in 1 mM L-NAME or 1 mM D-NAME in leech saline.

A drop in NO flux reflects a shallower gradient, stemming from either a lowered production at the source or an increased accumulation at the sink, but in fact there was little opportunity for accumulation of NO with time. Experiments were performed in a large bath and NO, a reactive molecule, could not accumulate. Furthermore, a drop in absolute current levels with time during the rapid transient decay was consistent with a decreased production at the source.

Statistics. To compare flux between treatments, a one-way ANOVA and Scheffe's test were performed. These same tests were used to compare the peak fluxes for each experiment, the mean half-life of the NO efflux for various treatments, and the kilocounts per minute from each citrulline assay. Nonlinear regression analysis was performed to determine the decay of the injury-induced NO efflux. Data were analyzed, and curves were fit with SigmaPlot 5.0 (SPSS, Chicago, IL). Statistical analysis of the R correlation coefficients was performed using a Student's t test and one-way factorial ANOVA in Statview 512.

RESULTS

Injury increased citrulline, reflecting injury-induced NO production

The standard citrulline assay revealed NO production 30 min after injury to the leech CNS by measuring the conversion of [^{3}H]arginine to [^{3}H]citrulline, which generated NO mole for mole. In the experimental group, cords were mechanically injured between ganglia and incubated 30 min in physiological saline before being processed further. Controls were uncrushed cords. For each experiment, citrulline counts from blank controls with no tissue extract were subtracted from each treatment. As a negative control, crushed cords were treated with 1 mM L-NAME. After calculation of the mean based on five replicate experiments for each treatment, the following counts were obtained: crush, $2.23 \pm 0.58 \times 10^5$ cpm; uncrushed controls, $3.67 \pm 2.73 \times 10^4$ cpm; and positive controls (rat cerebellum extract), $9.24 \pm 0.91 \times 10^4$ cpm. There was a significant difference between the citrulline counts of crushed cords compared with uncrushed cords, as determined by a one-way ANOVA and Scheffe's test [$F_{(2,12)} = 6.436$; $p < 0.01$] (Fig. 3). The citrulline counts of the crushed cords were higher than the citrulline counts of the positive control, which was a rat cerebellum extract having NOS activity (Bredt and Snyder, 1990). The increased citrulline counts in crushed cords as compared with uncrushed cords support the hypothesis that injury causes an increase in NOS activity and consequent NO production.

Injury causes a rapid transient efflux of nitric oxide from the nerve cord

To determine directly the NO fluxes caused by mechanical injury to the nerve cord, the current of the electrode polarized to 0.9 V

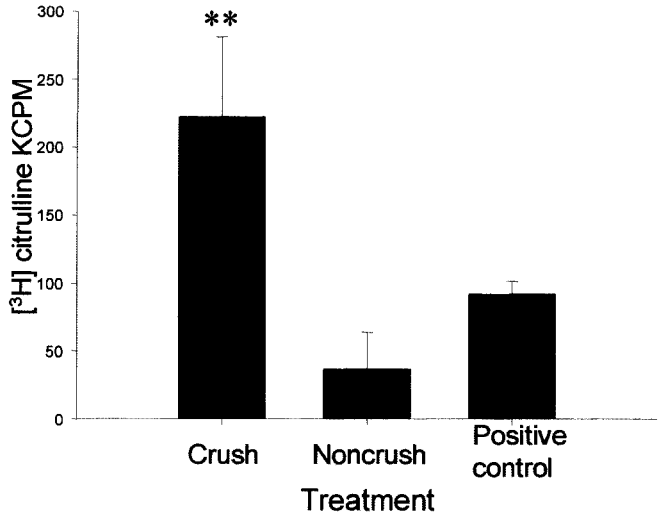

Figure 3. Injury to the leech CNS causes an increase in citrulline, reflecting NO production. In the experimental group, cords were injured and incubated in Ringer's for 30 min before being processed in the citrulline assay. Uncrushed controls were exposed and incubated for 30 min before being processed in the citrulline assay. Citrulline counts from blank controls were subtracted from each treatment. Statistical analysis of five experiments indicated that there was a statistical difference, with 95% confidence, according to Scheffe's test, between the citrulline counts of crushed and uncrushed cords [$DF_{(2,12)} = 6.436$, $p < 0.01$]. *KCPM*, 1000 cpm.

was measured differentially between two points at the lesion. The differential current was converted into a directional measurement of flux using the Fick equation. The translational movement of the microelectrode as a square wave helped assure that it was self-referencing; calibration was determined using artificial gradients of NO over a range of concentrations. Baseline currents were recorded at nerve cords that then were focally crushed, and the resulting increased currents were measured. From the change in NO concentration over a given distance, a static measurement of nitric oxide flux was calculated using the Fick equation within the gradient to measure the flux.

Crushing caused a rapid and transient efflux of NO, as illustrated in Figure 4*A*, which shows a representative example of the NO efflux (pmol cm^{-2} sec^{-1}) as a function of time after crushing. This pattern of response after injury was consistently observed for all experiments performed on fresh tissue. The mean peak injury-induced NO efflux of these initial injury experiments was calculated to be 803 ± 99 fmol cm^{-2} sec^{-1} ($n = 8$). Integration of all the flux versus time graphs for these experiments, performed in physiological saline, indicated that the injury caused ~200 pmol NO cm^{-2} to be produced within 30 min (Fig. 5).

The duration of this injury response was assessed by mathematically modeling the data. Mathematical analysis indicated that the injury-induced NO efflux could be well described by a single exponential decay model with a constant y term, given by the equation $f(t) = y_o + ae^{-t/\tau}$, with $y_o = 15.8 \pm 4.5$ fmol cm^{-2} sec^{-1}, $a = 787 \pm 99$ fmol cm^{-2} sec^{-1}, and $\tau = 117 \pm 30$ sec. Nonlinear regression analysis indicated the mean correlation coefficient (R) for the data from the control injury experiments (in physiological saline) was 0.948 ± 0.015. Some of the large SEs for the exponential decay constant (a) can be attributed to the difference in time between injuring the cord and actually starting measurement with the probe. These results indicate that after injury, there is a large and transient initial NO efflux accompanied by a lingering component.

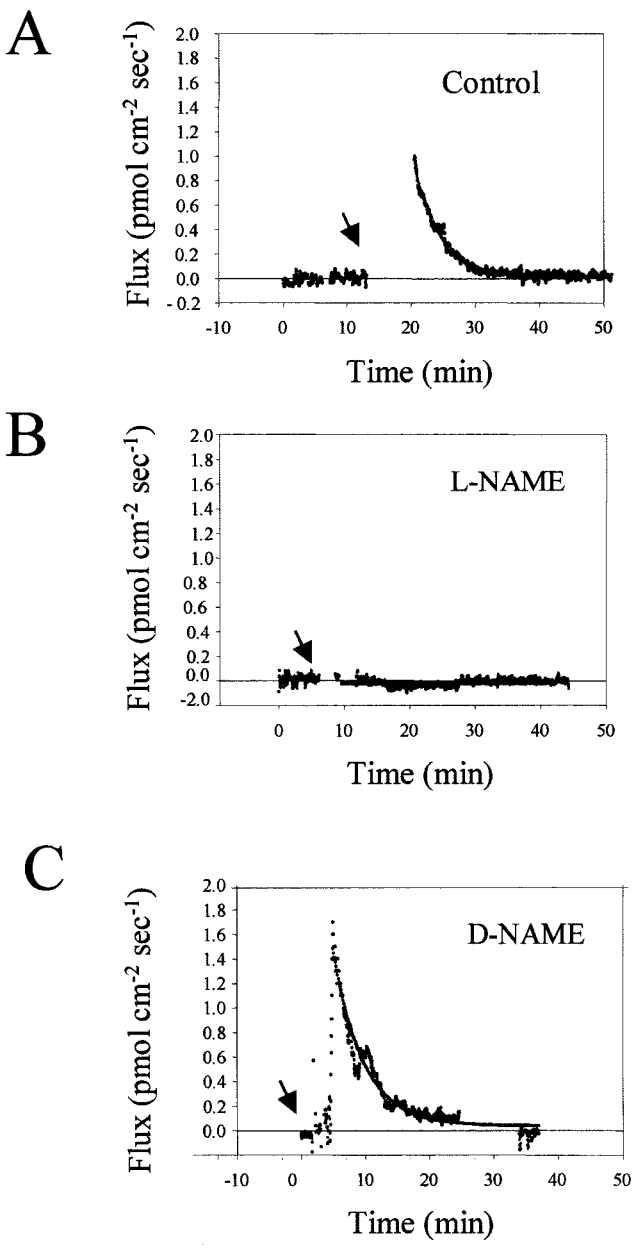

Figure 4. Injury causes NO efflux generated by NOS at the lesion. *A*, Representative response of the nerve cord to injury in physiological saline at time indicated by *arrows*. Differential current measured by the self-referencing probe, converted to flux (vertical axis, see Materials and Methods), jumped abruptly after injury. The mean peak efflux was 803 ± 99 fmol cm^{-2} sec^{-1}($n = 8$). All data were modeled to the equation $y = Y_0 \pm ae^{-bt}$. Modeled data are represented by the *solid line*. *B*, Representative response to injury (*arrow*) in saline containing 1 mM L-NAME. *C*, Same as *B*, but in 1 mM D-NAME. Treatment with 1 mM L-NAME reduced the injury response to a mean peak efflux of 199 ± 20 fmol NO cm^{-2} sec^{-1} ($n = 11$), whereas treatment with the inert enantiomer (D-NAME) resulted in a mean peak efflux of 1888 ± 773 fmol cm^{-2} sec^{-1} ($n = 6$). Results with L-NAME and D-NAME controls illustrate that the injury-induced response is caused specifically by the efflux of NO that is generated by NOS.

NO efflux is significantly reduced in NOS inhibitor L-NAME

Indirect evidence indicates that NO produced at the injury is generated by NOS that is sensitive to the NOS inhibitor L-NAME (Shafer et al., 1998; Furmanski et al., 1999). This implies that

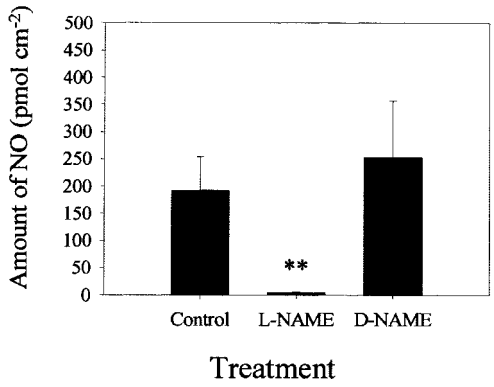

Figure 5. Injury-induced NO is blocked by NOS inhibition. Integration over time of the flux versus time graphs for each treatment gives the amount of NO produced at the lesion expressed as fmol NO cm^{-2} after crushing. Treatments were with physiological saline alone (control), in 1 mM L-NAME (a concentration that inhibits NOS isoforms), and in D-NAME as another control. Comparisons between treatments indicated that L-NAME significantly reduced (**) the NO produced during control injury experiments in physiological saline alone [one-way ANOVA, 95% confidence, Scheffe's test, $F_{(2,11)} = 15.271$; $p < 0.001$] or during treatment with 1 mM D-NAME [one-way ANOVA, 95% confidence, Scheffe's test, $F_{(2,11)} = 15.271$; $p < 0.001$].

incubation of the nerve cord in 1 mM L-NAME should reduce the injury-induced current by inhibiting NO production. To test this, nerve cords were dissected in 1 mM L-NAME, and measurements were made in that solution. Treatment with 1 mM L-NAME reduced the mean peak injury-induced efflux to 179 ± 3 fmol cm^{-2} sec^{-1} ($n = 11$). Integration of the flux over time showed that in the presence of L-NAME, the mean injury response dropped to 4.27 ± 1.9 pmol NO cm^{-2} (Fig. 5).

To verify that this reduction in response was not caused by a nonspecific toxic effect of L-NAME, parallel control experiments were performed with D-NAME, the inert enantiomer of L-NAME. In D-NAME, the injury-induced response was as large as that observed in initial, control injury experiments (Fig. 4*C*). The mean peak NO efflux in the presence of D-NAME was 2529 ± 585 fmol cm^{-2} sec^{-1} ($n = 6$). This D-NAME injury response was significantly greater, with 95% confidence, than the mean of the peak injury response in the presence of 1 mM L-NAME (110 ± 21 fmol cm^{-2} sec^{-1}) [$F_{(2,14)} = 13.082$; $p < 0.001$], but not significantly different from the mean peak response observed in the control injury experiments (803 ± 99 fmol NO cm^{-2} sec^{-1}) as determined by a one-way ANOVA and Scheffe's test, [$F_{(1,4)} = 4.024$; $p > 0.05$].

Integration of the NO flux in the D-NAME experiments gave ~250 pmol/mol NO cm^{-2} ($n = 6$) (Fig. 5). This NO production was significantly higher than that in 1 mM L-NAME, as determined by a one-way ANOVA and Scheffe's test [$F_{(2,11)} = 15.271$; $p < 0.01$]. There was also a significant difference between results from the control experiments and the L-NAME treatment, as determined by one-way ANOVA and Scheffe's test [$F_{(2,11)} = 15.271$; $p < 0.001$]. The data indicate that treatment with L-NAME attenuated the injury response by preventing formation of NO. Treatment with L-NAME also reduced the mean decay rate of the injury-induced NO efflux. In the presence of L-NAME, the injury-induced flux did not decay as rapidly as under the control injury experiments in normal Ringer's and the control D-NAME experiments. However, the L-NAME experiments did not fit the single exponential decay model as well as the control injury experiments and the D-NAME experiments. The mean R value for the control injury experiments was 0.948 ± 0.02, the R value for the D-NAME experiments was 0.98 ± 0.01, and the R value for the L-NAME experiments was 0.472 ± 0.18.

In three of six experiments, the L-NAME completely inhibited any NO production. For this reason, we calculated the mean τ value for the control injury experiments as 117 ± 30 sec and for the D-NAME experiments as 160 ± 60 sec, but we did not calculate the mean τ for the L-NAME experiments.

DISCUSSION

In this study, we have demonstrated with the use of a novel self-referencing NO-selective microelectrode that after injury to the leech CNS, there is rapid transient efflux of NO. Several techniques are currently available for the detection of NO, perhaps the most established being the citrulline assay (Bredt and Schmidt, 1996). This approach, although suitable for demonstrating the activity of NOS, has limited spatial and temporal resolution. To localize the production of NO with a spatial resolution of millimeters or micrometers, a microsensor is required.

The discovery of entirely separate components of NO efflux, including a hitherto unknown NO spike, is particularly novel. The smaller steady component was already known and accounts for previously described observations that persistent NO synthesis at the lesion stops microglia there, but the probe revealed a large transient component that could play a separate role, possibly activating microglia and thereby enabling them to migrate to the lesion. Some of the same features that have made the leech nervous system favorable for studies on synapse regeneration and microglia involvement in repair, such as its plain visibility and accessibility *in situ,* now provide new insights into the timing of NO generation in a system in which NO regulates cell movement involved in nerve repair.

Both the direct measurement using an NO-sensitive self-referencing microelectrode and indirect NO assay demonstrated an increase in NO production in the minutes after injury to the leech CNS, but the NO probe provided better temporal and spatial resolution. Injury-induced NO production began within minutes after injury, with a mean peak efflux that was transient, decreasing exponentially within minutes, but accompanied by a more slowly declining phase. Treatment of tissue with 1 mM L-NAME significantly reduced both the duration and amplitude of the injury response, whereas control treatment with the inert enantiomer D-NAME had no effect, indicating that NO was produced in response to the injury. Previous results showed that injury to the leech CNS activates eNOS in the large ensheathing glial cells and microglia of the connective (Shafer et al., 1998), consistent with the conclusion that these cells produce NO at the lesion. The nonlinear regression analysis confirmed that the injury response can be described by a large, rapidly decaying component, and then a slower, lingering component. This expands findings that injury-induced eNOS immunoreactivity occurs within minutes after injury and remains active long after (Chen et al., 2000).

The mean peak flux in D-NAME was higher than in the saline controls; however, this difference was not statistically significant. Because D-NAME is the inert enantiomer of L-NAME, it is not surprising that the injury response of the tissue in D-NAME was not significantly different from that of the control injury response. Because the value of NO efflux was in decline at the outset of measurements, there is uncertainty concerning the true peak efflux, which likely accounts for any apparent, insignificant difference from the controls. There were technical difficulties in mea-

suring the peak flux resulting from an inevitable delay between crushing and detection with the NO-selective microelectrode because the preparation had to be refocused under the inverted microscope attached to the NO-selective microelectrode after crushing (which was done with a separate dissecting microscope). Therefore, it is likely that we did not measure the entire NO efflux after injury and that the largest component of the NO spike remained undetected. Modifications in the experimental setup might permit measurement of a larger NO spike after injury than that detected in this study.

The reason for the drop in NO efflux from the crushed nerve cord is not understood, but it does not reflect a decline in substrate availability. A similar drop was observed both in saline and in Leibowitz-15 culture medium, in which L-arginine is abundant at 3 mM and is used to help buffer the medium, so it is not substrate limiting. In principle, NO efflux could drop although NO production is sustained. This might happen if barriers to NO efflux form or if NO scavengers (Zhao et al., 1999) are activated, although there is no indication that this occurs. One plausible explanation for the rapid drop in NO efflux after injury is that the downstream target of NO, soluble guanylate cyclase within the tissue, rapidly and specifically traps NO (Zhao et al., 1999).

The NO-mediated accumulation of microglia at the lesion may aid regeneration of the injured CNS axons because leech microglia not only phagocytize debris but also appear to deposit laminin along the pathway followed by axons as they grow through the lesion (von Bernhardi and Muller, 1995). Other studies support our hypothesis that NO is a stop signal for migrating microglia. In chick dorsal root ganglion explants, NO halted neurite motility (Hess et al., 1993) and collapsed growth cones in retinal ganglion cell explants (Rentería and Constantine-Paton, 1995). Microglia themselves contain NOS (Shafer et al., 1998). Although the large signal recorded with the NO probe would act only transiently on microglia, as those cells accumulate they might maintain the lingering signal recorded at the lesion.

REFERENCES

Balligand JL, Ungureanu-Longrois D, Simmons WW, Pimental D, Malinski TA, Kapturczak M, Taha Z, Lowenstein CJ, Davidoff AJ, Kelly RA, Smith TW, Michel T (1994) Cytokine-inducible nitric oxide synthase (iNOS) expression in cardiac myocytes. J Biol Chem 269:27580–27588.

Banati RB, Gehrmann J, Schubert P, Kreutzberg GW (1993) Cytotoxicity of microglia. Glia 7:111–118.

Brecknell JE, Fawcett JW (1996) Axonal regeneration. Biol Rev Camb Philos Soc 71:227–255.

Bredt DS, Schmidt HH (1996) The citrulline assay. In: Methods in nitric oxide research (Feelisch M, Stamler JS, eds), pp 249–270. New York: Wiley.

Bredt DS, Snyder SH (1990) Isolation of nitric oxide synthase, a calmodulin requiring enzyme. Proc Natl Acad Sci USA 87:682–685.

Cahill PS, Wightman RM (1995) Simultaneous amperometric measurement of ascorbate and catecholamine secretion from individual adrenal medullary cells. Anal Chem 67:2599–2605.

Chen A, Kumar SM, Sahley CL, Muller KJ (2000) Nitric oxide influences injury-induced microglial migration and accumulation in the leech CNS. J Neurosci 20:1036–1043.

Cobbs CS, Fenoy A, Bredt DS, Noble LJ (1997) Expression of nitric oxide synthase in the cerebral microvasculature after traumatic brain injury in the rat. Brain Res 751:336–338.

Fiallos-Estrada CE, Kummer W, Mayer B, Bravo R, Zimmermann M, Herdegen T (1993) Long-lasting increase of nitric oxide synthase immunoreactivity, NADPH-diaphorase reaction and cJUN co-expression in rat dorsal root ganglion neurons following sciatic nerve transection. Neurosci Lett 150:169–173.

Friedemann MN, Robinson SW, Gerhardt GA (1996) *O*-phenylendediamine-modified carbon fiber electrodes for the detection of nitric oxide. Anal Chem 1023:421–425.

Furmanski O, Kumar SM, Chen A, Einhorn B, Sahley CL, Muller KJ (1999) CNS injury rapidly induces eNOS immunoreactivity coincident with DAF-2A staining in *Hirudo medicinalis*. Soc Neurosci Abstr 25:1266.

Gevantman LH (1995) Handbook of chemistry and physics, Ed 76 (Lide DR, ed), p 63. Boca Raton, FL: CRC.

Hess DT, Patterson SI, Smith DS, Skene JH (1993) Neuronal growth cone collapse and inhibition of protein fatty acylation by nitric oxide. Nature 366:562–565.

Kuffler SW, Potter DD (1964) Glia in the leech central nervous system: physiological properties and neuron-glia relationship. J Neurophysiol 27:290–320.

Kumar SM, Porterfield DM, Muller KJ, Sahley CL, Smith PJS (1999) *In situ* measurement of injury-induced nitric oxide (NO). Soc Neurosci Abstr 25:313.

Land SC, Porterfield DM, Sanger RH, Smith PE (1999) The self-referencing oxygen selective microelectrode: detection of transmembrane oxygen flux from single cells. J Exp Biol 202:211–218.

Lander HM, Sehajpal PK, Novogrodsky A (1993) Nitric oxide signaling: a possible role for G proteins. J Immunol 151:7182–7187.

Lantoine F, Iouzalen L, Devynck M, Millanvoye-van Brussel E, David-Dufilho M (1998) Nitric oxide production in human endothelial cells stimulated by histamine requires Ca^{2+} influx. Biochem J 330:695–699.

Malinski T, Taha Z (1992) Nitric oxide release from a single cell measured *in situ* by a porphyrinic-based microsensor. Nature 358:676–678.

Malinski T, Radomski MW, Taha Z, Moncada S (1993) Direct electrochemical measurement of nitric oxide released from human platelets. Biochem Biophys Res Commun 194:960–965.

Modney BK, Sahley CL, Muller KJ (1997) Regeneration of a central synapse restores non-associative learning. J Neurosci 17:6478–6482.

Nicholls JG (1987) The search for connections: study of regeneration in the nervous system of the leech. In: Magnes Lecture Series, Vol II, pp 1–84. Sunderland, MA: Sinauer.

Nicholls JG, Baylor DA (1968) Specific modalities and receptive fields of sensory neurons in the CNS of the leech. J Neurophysiol 31:740–756.

Porterfield DM, Laskin JD, Malchow RP, Billack B, Smith PJS, Heck DE (2000) Direct measurement of nitric oxide fluxes from macrophages using a novel self-referencing electrode. Am J Physiol, in press.

Rentería RC, Constantine-Paton M (1995) Exogenous nitric oxide causes collapse of retinal ganglion cell axonal growth cones vitro. J Neurobiol 29:415–428.

Shafer OT, Chen A, Kumar SM, Muller KJ, Sahley CL (1998) Injury-induced expression of endothelial nitric oxide synthase by glial and microglial cells in the leech central nervous system within minutes after injury. Proc R Soc Lond B Biol Sci 265:2171–2175.

Silverton SF, Mesaros S, Markham GD, Malinski T (1995) Osteoclast radical interactions: NADPH causes pulsatile release of NO and stimulates superoxide production. Endocrinology 136:5244–5247.

Smith PJS (1995) The non-invasive probes: tools for measuring transmembrane ion flux. Nature 378:645–646.

Smith PJS, Hammar K, Porterfield DM, Sanger RH, Trimarchi JR (1999) A self-referencing, non-invasive, ion selective electrode for single cell detection of trans-plasma membrane calcium flux. Microsc Res Tech 46:398–417.

Tschudi MR, Barton M, Bersinger NA, Moreau P, Cosentino F, Noll G, Malinski T, Lüscher TF (1996) Effect of age on kinetics of nitric oxide release in rat aorta and pulmonary artery. J Clin Invest 98:899–905.

Vizzard MA, Erdman SL, de Groat WC (1995) Increased expression of neuronal nitric oxide synthase (NOS) in visceral neurons after nerve injury. J Neurosci 15:4033–4045.

von Bernhardi R, Muller KJ (1995) Repair of the central nervous system: lessons from lesions in leeches. J Neurobiol 27:353–366.

Yu WH (1997) Regulation of nitric oxide synthase expression in motorneurons following nerve injury. Dev Neurosci 19:247–254.

Zhao Y, Brandish PE, Ballou DP, Marletta MA (1999) A molecular basis for nitric oxide sensing by soluble guanylate cyclase. Proc Natl Acad Sci USA 96:14753–14758.